Gold-Mediated Exfoliation of Ultralarge Optoelectronically-Perfect Monolayers

*Sujay B. Desai, Surabhi R. Madhvapathy, Matin Amani, Daisuke Kiriya, Mark Hettick, Mahmut Tosun, Yuzhi Zhou, Madan Dubey, Joel W. Ager III, Daryl Chrzan, and Ali Javey**

Transition-metal dichalcogenides (TMDCs) are a class of layered materials analogous to graphene, which have aroused immense interest in the last few years as a potential platform for future electronic and optoelectronic applications.[1,2] The layers in these materials are held together by weak van der Waals (vdW) forces, making it easy to cleave them to the limit of a monolayer (a single unit of three atomic layers, comprised of one layer of transition metal atoms sandwiched between two layers of chalcogen atoms). Monolayers of many TMDCs, such as MoS_2, WS_2, WSe_2, and $MoSe_2$, are especially exciting since they are direct band gap semiconductors, making them ideal for applications in devices such as light-emitting diodes (LEDs), lasers, photodiodes, etc. Their naturally passivated surfaces, sizeable bandgaps (≈1–2 eV), atomic scale thickness (≈0.7 nm), and low dielectric constant (≈4) also make them suitable candidates for replacing silicon at the metal-oxide-semiconductor field-effect transistor (MOSFET) scaling limit due to mitigated short channel effects.[3]

Monolayer-TMDC flakes typically produced using the tape exfoliation method (similar to Scotch® tape method used for graphene[4]) are small in size (≈5 µm) and the yield of the procedure is poor. Simple modifications like exfoliating the flakes on a hot plate result in a slight increase in the size of flakes achieved.[5] Tape exfoliation of monolayers relies on the probability of cleaving the crystal such that $(N-1)$ layers remain adhered to the tape while only a monolayer is transferred onto the SiO_2 substrate. The interaction of TMDCs with the SiO_2 substrate is weak, resulting in a low probability of the above event and, consequently, minimal control over the flake size. The small size of the exfoliated flakes makes their characterization difficult. Techniques such as angle-resolved photoemission spectroscopy (ARPES), X-ray diffraction (XRD), and X-ray photoelectron spectroscopy (XPS), etc., which require large-area macroscopic samples, are difficult to apply to small monolayer samples. Small flakes from the tape exfoliation method also limit the size of electronic devices and circuits, which can be fabricated per flake to just a few transistors.[6]

In this work, we demonstrate an exfoliation technique using evaporated gold films[7,8] to exfoliate large area TMDC monolayers onto various substrates such as SiO_2/Si and quartz. Gold is known to have a strong affinity for chalcogens, especially to sulfur atoms with which it forms a semicovalent bond with bond strength of ≈45 kcal mol^{-1}.[9,10] The interaction between gold and sulfur has been used in the formation of self-assembled monolayers of thiolated organic molecules on gold surfaces[10] and gold–thiolate complexes. The same idea is used in this work by selectively increasing the adhesion of the topmost layer of a bulk TMDC crystal to gold by evaporating a thin film on it and subsequently peeling it off from the bulk crystal.

The detailed process flow is illustrated in **Figure 1**a. Gold (≈100–150 nm) is evaporated onto bulk MX_2 (M = Mo or W; X = S or Se) crystals. The gold atoms bond with the chalcogen atoms of the topmost layer of MX_2. The interaction of the topmost layer with the evaporated gold is stronger than the vdW interactions of that same layer with the bottom layers of MX_2. This enables selective peel-off of the topmost layer using a thermal release tape which is later stuck onto the desired target substrate (SiO_2/Si or quartz). The thermal tape is then released on a hot plate (≈130 °C) and the substrate is treated with a mild O_2 plasma to remove the tape residue from the surface. The O_2 plasma power and etching time are kept low to ensure that the gold is not etched away, thereby exposing the underlying monolayer MX_2. The gold film is then etched using potassium iodide and iodine (KI/I_2) wet etch (Transene Gold Etch—type TFA for 4 min), which does not etch the TMDC flakes. This is followed by a 10 min acetone clean and isopropyl alcohol (IPA) rinse to remove any residues and obtain the large-area monolayers.

The relatively strong binding of the gold to the topmost layer of MX_2 enhances the probability of the crystal to cleave right at the topmost layer, increasing both the yield and the

S. B. Desai, S. R. Madhvapathy, M. Amani, Dr. D. Kiriya, M. Hettick, M. Tosun, Prof. A. Javey
Electrical Engineering and Computer Sciences
University of California
Berkeley, CA 94720, USA
E-mail: ajavey@eecs.berkeley.edu

S. B. Desai, S. R. Madhvapathy, M. Amani, Dr. D. Kiriya, M. Hettick, M. Tosun, Prof. J. W. Ager III, Prof. D. Chrzan, Prof. A. Javey
Materials Sciences Division
Lawrence Berkeley National Laboratory
Berkeley, CA 94720, USA

S. B. Desai, M. Amani, Dr. D. Kiriya, M. Hettick, M. Tosun, Prof. A. Javey
Berkeley Sensor and Actuator Center
University of California
Berkeley, CA 94720, USA

Y. Zhou, Prof. J. W. Ager III, Prof. D. Chrzan
Materials Science and Engineering Department
University of California
Berkeley, CA 94720, USA

Dr. M. Dubey
Sensors and Electronic Devices Directorate
US Army Research Laboratory
Adelphi, MD 20723, USA

DOI: 10.1002/adma.201506171

ADVANCED MATERIALS
www.advmat.de

www.MaterialsViews.com

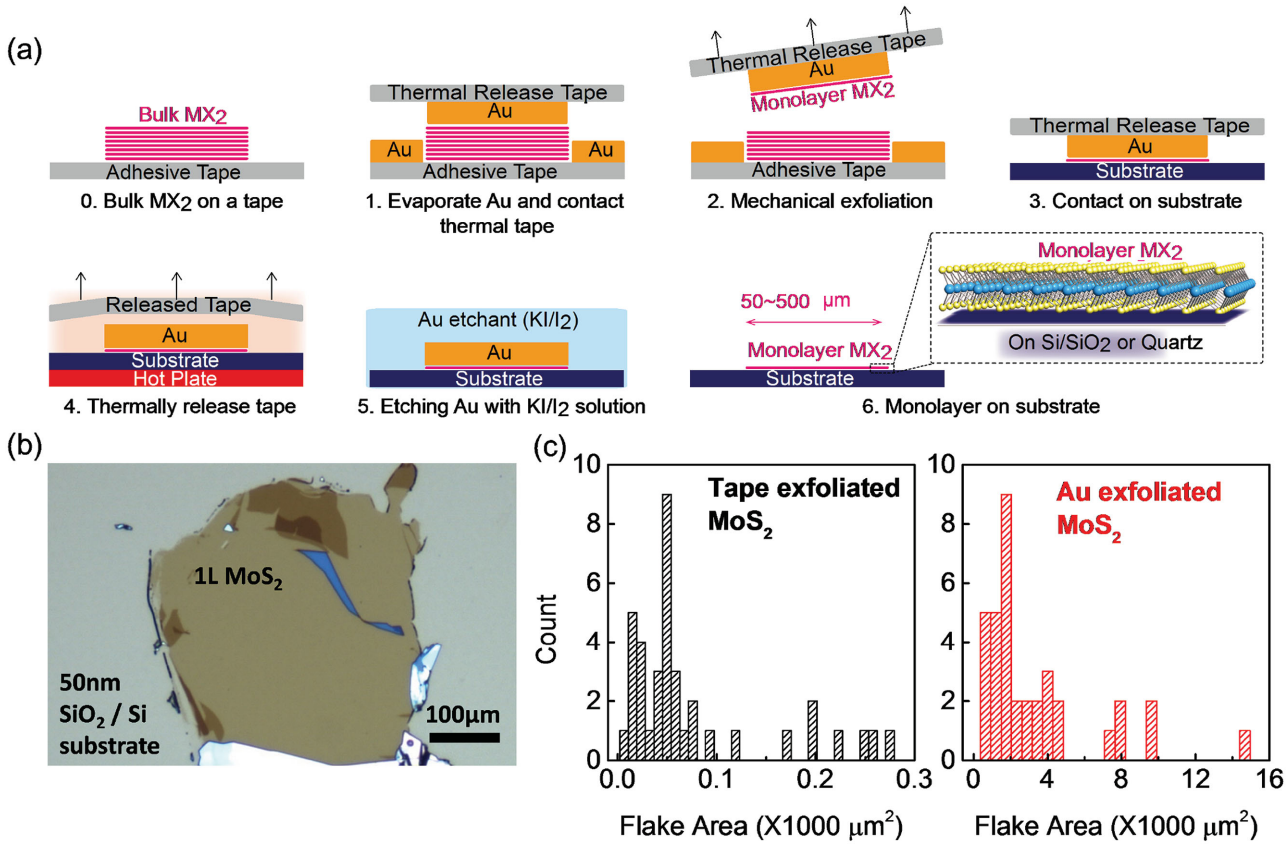

Figure 1. a) Schematic illustration of the Au exfoliation process. b) Optical microscope image of a large monolayer MoS_2 flake. c) Histogram of flake areas for tape-exfoliated versus Au-exfoliated MoS_2.

size of the flakes obtained. Using this technique, large area MoS_2 monolayers with lateral dimensions up to ≈500 μm are obtained. Figure 1b shows the optical image of one such large monolayer on a 50 nm SiO_2/Si substrate. The process was also used to exfoliate other TMDCs such as WS_2 and WSe_2 (Figure S1b,c, Supporting Information). For the scope of this paper, we focus on the exfoliation and characterization of MoS_2 as a model system for all TMDCs. The histograms in Figure 1c show that the flake area for MoS_2 flakes obtained by the gold (Au) exfoliation method is ≈10,000 times larger than that of flakes obtained by the tape exfoliation method. The size of the monolayer flakes exfoliated by gold is primarily limited by the size of the source MoS_2 crystal domains and may be increased in the future by the use of large sized flat crystals. Figure S2 (Supporting Information) shows the optical microscope images of several Au-exfoliated MoS_2 samples on 50 nm SiO_2/Si substrates. The images indicate that exfoliated monolayer area is larger than that of multilayer MoS_2, thereby demonstrating that Au adheres preferentially to the topmost layer of MoS_2. The exfoliated bulk regions may be attributed to cleaving at potential defect sites in the source crystal. Also, we empirically observed that the probability of obtaining Au-exfoliated monolayers is several times more compared to the tape exfoliation method. The exfoliation method described here does not involve the double transfer of exfoliated monolayers like the technique in ref.,[7] which first requires exfoliation onto an Au substrate followed by transfer to the target substrate. Furthermore, the flakes are uniform over a large area which is important for electrical device applications.

The success of the Au mediated exfoliation of large-area MoS_2 can be attributed to two main factors. First, as noted above, the Au binds to the S atoms quite strongly which enables its adhesion to the topmost layer of MoS_2. A second factor also contributes to the single layer selectivity of the process: as shown by previous calculations, large mismatch in lattice constants causes strain in the topmost layer of MoS_2 and gold.[11] The first layer of MoS_2 is compliant and can slip relative to the underlying substrate, which slightly weakens its bond with the other layers of the bulk MoS_2 crystal. Similarly, strain due to evaporated metal films was also used to exfoliate single layer graphene as shown in ref.[11]

Prior to this work, because of the small size of tape-exfoliated flakes, surface characterization of MoS_2 monolayers has only been possible with photoemission electron microscopy (PEEM).[12] Gold-exfoliated monolayers are sufficiently large to be characterized by standard XPS measurements. XPS measurements were performed using a macroscale monochromatic Al Kα excitation source and allowed direct comparison of the monolayers to the bulk crystal used for our source material (**Figure 2**). Following background subtraction and fitting (details given in the Experimental Section), the XPS data for monolayer MoS_2 is found to be qualitatively similar to the XPS spectrum of MoS_2 bulk crystal with some notable differences in the peak binding energies. Of particular note is the

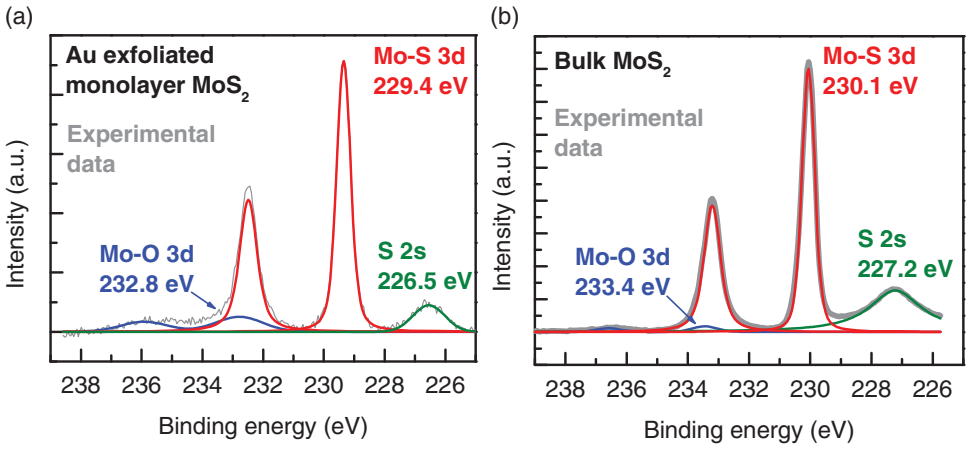

Figure 2. a) XPS experimental data and fitted Voigt curves for a Au-exfoliated monolayer MoS_2. b) XPS experimental data and fitted curves for the bulk MoS_2 crystal source.

redshift (≈0.7 eV) in the binding energy for monolayer MoS_2 compared to bulk MoS_2. This is consistent with charge transfer from the underlying silicon substrate to the monolayer MoS_2 flake. This XPS measurement demonstrates the importance of the Au exfoliation technique toward accelerating monolayer TMDC research since measurements such as PEEM, require bright light sources which are typically limited to synchrotron facilities.

The Au-exfoliated MoS_2 flakes undergo a multistep process, including Au evaporation, KI/I_2 etching, and acetone cleaning. Apart from XPS, careful characterization by optical and electrical measurements is necessary to compare their quality to flakes from the tape exfoliation method. **Figure 3**a,b shows that the Raman and photoluminescence (PL) spectra for Au-exfoliated MoS_2 flakes are identical to those of tape-exfoliated MoS_2 flakes. No new features or peaks are observed in both Raman and PL. Identical Raman peak positions also indicate that the flakes are not strained. Figure 3c,d shows that the Raman map of the position of the E^1_{2g} and the A_{1g} peaks of MoS_2 for the large flake are shown in Figure S1a (Supporting Information). The Raman peak position value can be used to identify the monolayer and multilayer MoS_2 regions of the flake.[13] The peak positions are quite uniform over the entire area of the monolayer flake away from any markers on the chip. Near the markers (5/35 nm thick Cr/Au) we see a slight variation in the peak position indicating that the MoS_2 locally is strained

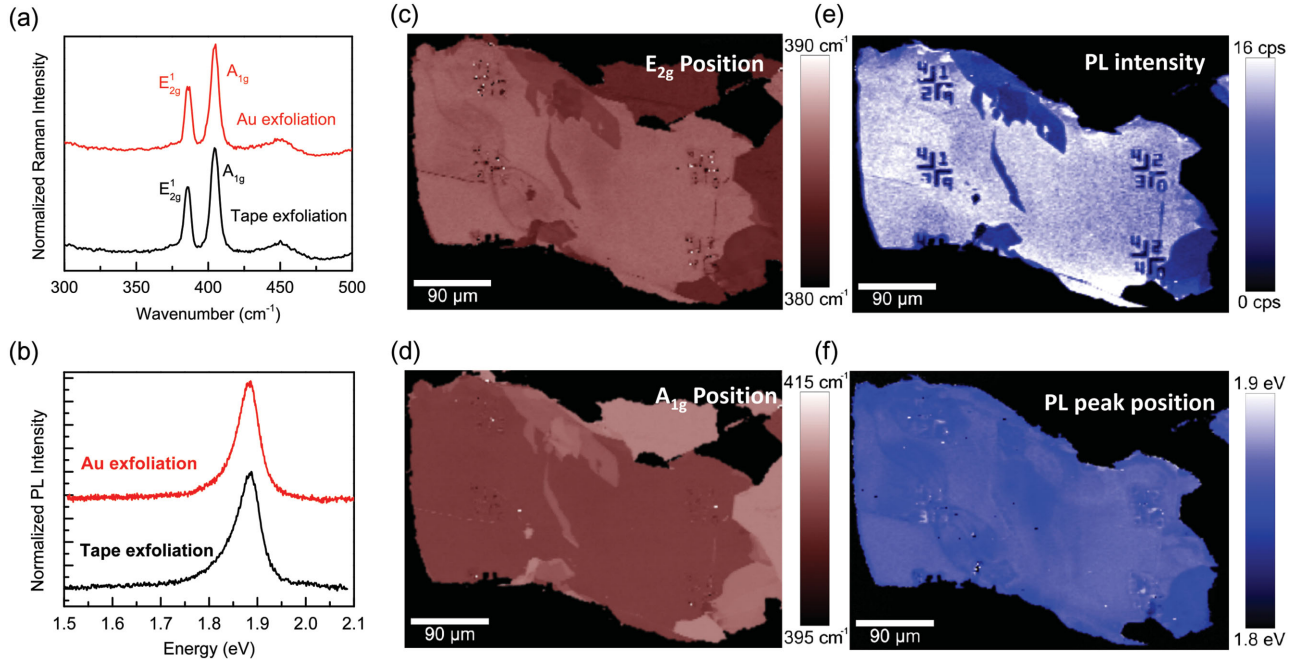

Figure 3. a) Raman spectra comparison for Au-exfoliated flake versus tape-exfoliated flake. b) Photoluminescence spectra comparison for Au-exfoliated flake versus tape-exfoliated flake. c,d) Raman peak E^1_{2g} and A_{1g} maps of monolayer MoS_2 flake in Figure S1a (Supporting Information). e,f) PL peak intensity and position maps of monolayer MoS_2 flake in Figure S1a (Supporting Information).

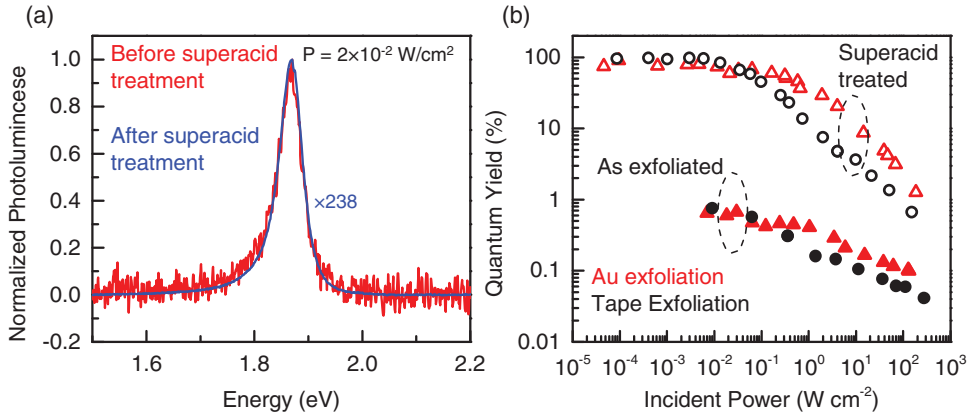

Figure 4. a) PL spectra before and after chemical treatment on Au-exfoliated monolayer MoS_2. b) Quantum yield versus incident power intensity for tape-exfoliated[15] and Au-exfoliated monolayer MoS_2 before (as exfoliated) and after chemical treatment (TFSI).

due to substrate topography.[14] Figure 3e,f shows the PL peak position and intensity map for the same flake. This map is also quite uniform over the entire monolayer region except for the strain fields near the markers which is visible in the PL peak position map. The absence of strain and the uniformity of Raman and PL over the large area of MoS_2 is of utmost significance for device applications. Strain induced variations of the bandgap, mobility and effective mass can all affect device performance, resulting in statistical variations of intrinsic parameters like threshold voltage, ON/OFF current, etc., similar to problems caused by line-edge roughness in modern MOSFETs.

Photoluminescence quantum yield (QY) measurements, which provide a quantitative estimate of the fraction of radiative recombination in a material over total recombination, are an accurate way to gauge optoelectronic quality. For an ideal material with zero defects (i.e., trap states) and low carrier concentration the QY should be 100% at low injection levels where carrier–carrier interactions, such as Auger or biexcitonic recombination, are not dominant. However, it has been experimentally found that the tape-exfoliated MoS_2 flakes have poor QY of the order of ≈1% at most[2] due to defects such as vacancies preexisting in the bulk crystal. Recently, we demonstrated that it is possible to repair/passivate defects in tape-exfoliated MoS_2 flakes using bis(trifluoromethane)sulfonimide (TFSI, Sigma-Aldrich), an organic superacid, leading to a drastic enhancement in QY to almost 100%.[15] The same treatment procedure is applied here to the Au-exfoliated large-area MoS_2 flakes. **Figure 4**a shows the PL spectrum for the Au-exfoliated monolayer MoS_2 before and after the chemical treatment. The PL intensity increased by a factor of ≈238× after treatment for this sample. Figure 4b shows the QY measured over a pump-power dynamic range of six orders of magnitude for both tape-exfoliated (from ref.[15]) and Au-exfoliated MoS_2 monolayers, before and after the chemical treatment. The details of the measurement are provided in ref.[15]. The chemical treatment results in almost 100% internal QY, yielding ultralarge optoelectronically perfect monolayer flakes at low pump-power as was observed previously in tape-exfoliated samples. Furthermore, at higher injection levels we observe a reduction in the QY consistent with intrinsic biexcitonic recombination which was observed in tape-exfoliated flakes; both samples show the onset of biexcitonic recombination at similar pump-power. These observations suggest that the optical quality, defect type, and defect passivation mechanism are similar for MoS_2 flakes obtained from both exfoliation methods.

Electrical characterization of Au-exfoliated monolayer MoS_2 was performed to comprehensively compare its quality against tape-exfoliated flakes and extract important device parameters such as mobility. **Figure 5**a shows the cross-section schematic of a back-gated monolayer MoS_2 MOSFET fabricated on 50 nm SiO_2/n^{++} Si substrate with Ni source and drain contacts. Figure 5b is a representative image of fabricated monolayer MoS_2 devices with varying channel lengths. The arbitrarily shaped monolayer MoS_2 flakes are pattern etched into a regular shape channel to ensure deterministic current flow from source to drain thereby permitting accurate extraction of device parameters. Details of the device fabrication are described in the Experimental Section. Figure 5c,d shows the I_D–V_{GS} and I_D–V_{DS} characteristics for a long channel (L = 20 µm) device measured in vacuum. The Si substrate is used as the global back gate with the 50 nm SiO_2 layer serving as the gate dielectric. The electrical characteristics show typical long channel MOSFET behavior with saturation observed in the I_D–V_{DS} characteristics.

After accounting for the large contact resistance (R_C) which leads to a huge underestimation of mobility of carriers as described in ref.,[16] the mobility for electrons is calculated to be ≈26 $cm^2\ V^{-1}\ s^{-1}$ for the L = 20 µm monolayer MoS_2 device in Figure 5c,d ($R_C \approx 3.85$ MΩ µm, $(V_G - V_T) \approx 6$ V). The value of extracted mobility is consistent with the range of values reported in literature for monolayer MoS_2.[17] The electrical characteristics of Au-exfoliated flakes are thus found to be similar to those of monolayer MoS_2 flakes from tape exfoliation. The long channel length MOSFETs (L = 20 and 30 µm) further demonstrate the uniformity of the monolayer MoS_2 flakes over a large area which is essential for building complex circuits.

In conclusion, we have demonstrated an exfoliation technique utilizing the interaction strength of Au with chalcogens to preferentially obtain large areas of monolayer TMDCs on various substrates with high yield compared to the standard tape exfoliation method. Through extensive electrical and

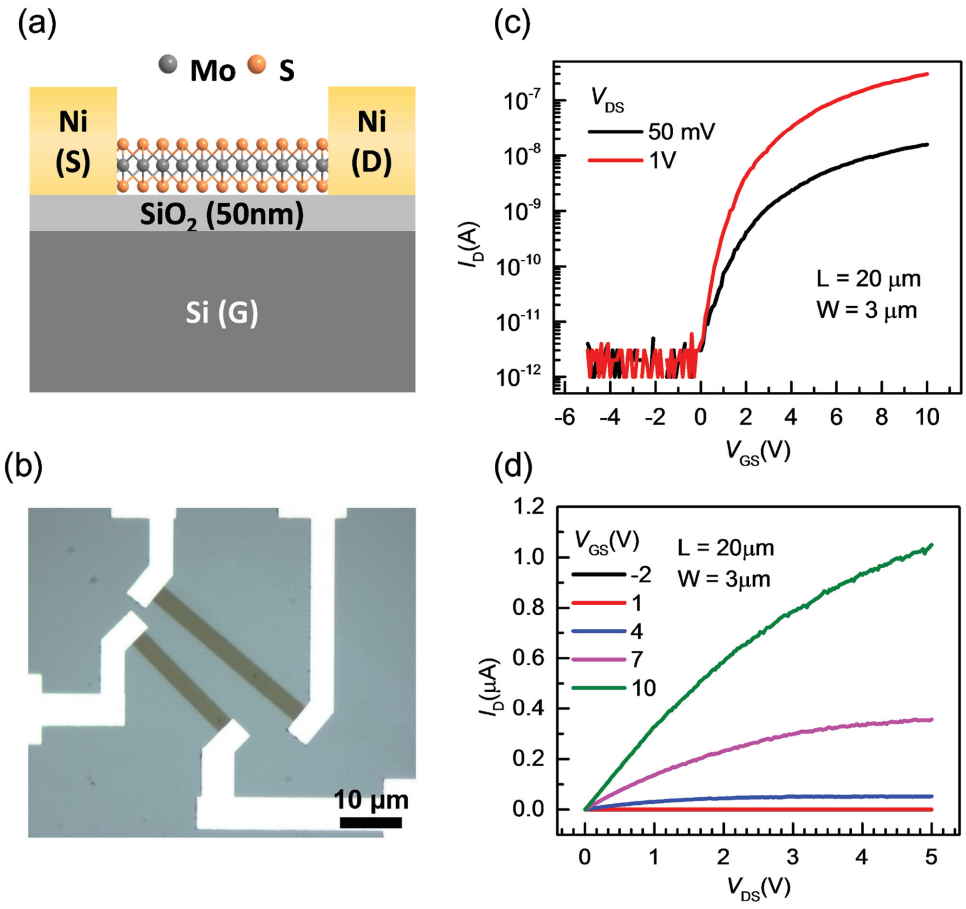

Figure 5. a) Schematic illustration of a monolayer MoS_2 back-gated MOSFET. b) Representative completed device post-MoS_2 patterned etching and contact formation. c,d) I_D–V_{GS} and I_D–V_{DS} data for $L = 20$ μm, $W = 3$ μm device, respectively.

optical characterization we conclude that the quality of flakes obtained by the tape exfoliation and by the Au exfoliation techniques is the same. Ultralarge optoelectronically perfect MoS_2 monolayers with a PL QY of ≈100% were obtained after treatment with an organic superacid. Standard XPS performed on ultralarge area monolayer MoS_2 illustrates the importance of this technique for expanding research capabilities. Automating and mechanizing the transfer process described in this work may be explored in the future for more controlled exfoliation and transfer of TMDC monolayers onto desired substrates. Ultimately, this technique can advance the possibility of large scale fabrication of monolayer TMDC devices.

Experimental Section

XPS Measurements: XPS measurements were performed on a Kratos AXIS Ultra-DLD (delay-line detector) spectrometer, using a monochromatic Al K-Alpha excitation source (spot size is 1 mm × 2 mm). Instrument work function was calibrated immediately prior to the measurement using a sputtered Au reference, utilizing the valence band Fermi edge and Au 4f position for the energy reference. Measurement of the bulk material was performed on a freshly exfoliated surface, using a slot aperture defining an area ≈700 μm × 300 μm. Measurement of a large (≈50 μm × 60 μm) monolayer, exfoliated by Au exfoliation method and transferred using a dry pick-and-place method[12] to the silicon analysis substrate, was performed using the same excitation source and pass energy resolution, and the field of view was limited to ≈400 μm × 400 μm by tuning of the electrostatic lens and use of a small area aperture. Charge correction for the MoS_2 samples was performed using the adventitious carbon C 1s peak position.[18]

Molybdenum and sulfur core level curve fits were performed using Voigt line shapes, with doublet spin orbit splitting area ratios defined to the normal 3:2 ratio for the 3d 5/2 and 3/2 components. Background subtraction was performed in combination with curve fits using the well-known Shirley background for the Au reference and MoS_2 bulk sample, and an alternative linear background for the monolayer. This alternate was necessary due to a more prominent linear background lineshape present in the Mo 3d and S 2s analysis area, likely due to substrate contributions to the spectra.

Raman and PL Mapping: High-resolution PL mapping was performed using a WITec Alpha 300RA equipped with a scanning stage. The sample was excited using the 532 nm line of a frequency-doubled Nd:YAG (neodymium-doped yttrium aluminium garnet) laser as the excitation source and focused on the sample using a 100× objective. The laser power is 2 μW with a diffraction-limited spot size. QY measurement conditions are described in ref.[15]

Sample Preparation for Photoluminescence Quantum Yield Measurements: For quantum yield measurements MoS_2 (SPI Supplies) was exfoliated on quartz (using Au exfoliation method). Monolayers were identified by optical contrast. Samples were treated using TFSI (Sigma-Aldrich) using the following preparation procedure: TFSI (20 mg) was dissolved in 1,2-dichloroethane (10 mL) (DCE, Sigma-Aldrich) to make a 2 mg mL^{-1} solution. The solution is further diluted with 1,2-dichlorobenzene (Sigma-Aldrich) or DCE to make a 0.2 mg mL^{-1}

TFSI solution. The sample was then immersed in the 0.2 mg mL^{-1} solution in a tightly closed vial for 10 min on a hot plate (100 °C). The sample was removed and blow-dried with nitrogen without rinsing and subsequently annealed at 100 °C for 5 min.

Electrical Device Fabrication: Electron-beam lithography is used to pattern an etch mask using poly(methyl) methacrylate (PMMA) C4 resist (MicroChem Corp.). XeF_2 etching[19] is used to then pattern the monolayer into long strips which form the channel region of the MOSFET. The resist is removed in acetone following which the source-drain contacts are patterned using electron-beam lithography. 40 nm Ni is evaporated using thermal evaporation followed by subsequent liftoff in acetone to form the contacts.

Supporting Information

Supporting Information is available from the Wiley Online Library or from the author.

Acknowledgements

S.B.D., S.R.M., and M.A. contributed equally to this work. This work was supported by the Electronics Materials program funded by the Director, Office of Science, Office of Basic Energy Sciences, Material Sciences and Engineering Division of the U. S. Department of Energy under Contract No. DE-AC02-05CH11231. XPS measurements were performed at the Joint Center for Artificial Photosynthesis (JCAP), a Department of Energy (DOE) Energy Innovation Hub, supported through the Office of Science of the U.S. Department of Energy under Award No. DE-SC0004993.

Received: December 11, 2015
Revised: January 25, 2016
Published online: March 23, 2016

[1] a) B. Radisavljevic, A. Radenovic, J. Brivio, V. Giacometti, A. Kis, *Nat. Nano* **2011**, *6*, 147; b) Q. H. Wang, K. Kalantar-Zadeh, A. Kis, J. N. Coleman, M. S. Strano, *Nat. Nano* **2012**, *7*, 699; c) M. Xu, T. Liang, M. Shi, H. Chen, *Chem. Rev.* **2013**, *113*, 3766; d) H. Fang, S. Chuang, T. C. Chang, K. Takei, T. Takahashi, A. Javey, *Nano Lett.* **2012**, *12*, 3788; e) S. Z. Butler, S. M. Hollen, L. Cao, Y. Cui, J. A. Gupta, H. R. Gutiérrez, T. F. Heinz, S. S. Hong, J. Huang, A. F. Ismach, E. Johnston-Halperin, M. Kuno, V. V. Plashnitsa, R. D. Robinson, R. S. Ruoff, S. Salahuddin, J. Shan, L. Shi, M. G. Spencer, M. Terrones, W. Windl, J. E. Goldberger, *ACS Nano* **2013**, *7*, 2898.

[2] K. F. Mak, C. Lee, J. Hone, J. Shan, T. F. Heinz, *Phys. Rev. Lett.* **2010**, *105*, 136805.

[3] P. Zhao, S. Desai, M. Tosun, T. Roy, H. Fang, A. Sachid, M. Amani, C. Hu, A. Javey, *IEEE IEDM Tech. Dig.* **2015**, 27.3.1.

[4] K. S. Novoselov, A. K. Geim, S. V. Morozov, D. Jiang, Y. Zhang, S. V. Dubonos, I. V. Grigorieva, A. A. Firsov, *Science* **2004**, *306*, 666.

[5] Y. Huang, E. Sutter, N. N. Shi, J. Zheng, T. Yang, D. Englund, H.-J. Gao, P. Sutter, *ACS Nano* **2015**, *9*, 10612.

[6] M. Tosun, S. Chuang, H. Fang, A. B. Sachid, M. Hettick, Y. Lin, Y. Zeng, A. Javey, *ACS Nano* **2014**, *8*, 4948.

[7] G. Z. Magda, J. Pető, G. Dobrik, C. Hwang, L. P. Biró, L. Tapasztó, *Sci. Rep.* **2015**, *5*, 14714.

[8] C.-L. Hsu, C.-T. Lin, J.-H. Huang, C.-W. Chu, K.-H. Wei, L.-J. Li, *ACS Nano* **2012**, *6*, 5031.

[9] a) H. Grönbeck, A. Curioni, W. Andreoni, *J. Am. Chem. Soc.* **2000**, *122*, 3839; b) E. Pensa, E. Cortés, G. Corthey, P. Carro, C. Vericat, M. H. Fonticelli, G. Benítez, A. A. Rubert, R. C. Salvarezza, *Acc. Chem. Res.* **2012**, *45*, 1183.

[10] H. Hakkinen, *Nat. Chem.* **2012**, *4*, 443.

[11] a) Y. Zhou, D. Kiriya, E. E. Haller, J. W. Ager III, A. Javey, D. C. Chrzan, *Phys. Rev. B* **2016**, *93*, 054106; b) J. Kim, H. Park, J. B. Hannon, S. W. Bedell, K. Fogel, D. K. Sadana, C. Dimitrakopoulos, *Science* **2013**, *342*, 833.

[12] H. Fang, C. Battaglia, C. Carraro, S. Nemsak, B. Ozdol, J. S. Kang, H. A. Bechtel, S. B. Desai, F. Kronast, A. A. Unal, G. Conti, C. Conlon, G. K. Palsson, M. C. Martin, A. M. Minor, C. S. Fadley, E. Yablonovitch, R. Maboudian, A. Javey, *Proc. Natl. Acad. Sci. USA* **2014**, *111*, 6198.

[13] K.-K. Liu, W. Zhang, Y.-H. Lee, Y.-C. Lin, M.-T. Chang, C.-Y. Su, C.-S. Chang, H. Li, Y. Shi, H. Zhang, C.-S. Lai, L.-J. Li, *Nano Lett.* **2012**, *12*, 1538.

[14] a) S. B. Desai, G. Seol, J. S. Kang, H. Fang, C. Battaglia, R. Kapadia, J. W. Ager, J. Guo, A. Javey, *Nano Lett.* **2014**, *14*, 4592; b) H. J. Conley, B. Wang, J. I. Ziegler, R. F. Haglund, S. T. Pantelides, K. I. Bolotin, *Nano Lett.* **2013**, *13*, 3626.

[15] M. Amani, D.-H. Lien, D. Kiriya, J. Xiao, A. Azcatl, J. Noh, S. R. Madhvapathy, R. Addou, S. KC, M. Dubey, K. Cho, R. M. Wallace, S.-C. Lee, J.-H. He, J. W. Ager, X. Zhang, E. Yablonovitch, A. Javey, *Science* **2015**, *350*, 1065.

[16] a) A. B. Sachid, F. Hui, A. Javey, H. Chenming, presented at Int. Symp. VLSI Technol. Syst. Appl., Hsinchu, Taiwan, April **2014**; b) T. Roy, M. Tosun, J. S. Kang, A. B. Sachid, S. B. Desai, M. Hettick, C. C. Hu, A. Javey, *ACS Nano* **2014**, *8*, 6259.

[17] a) H. Fang, M. Tosun, G. Seol, T. C. Chang, K. Takei, J. Guo, A. Javey, *Nano Lett.* **2013**, *13*, 1991; a) B. Radisavljevic, A. Kis, *Nat. Mater.* **2013**, *12*, 815.

[18] NIST X-ray Photoelectron Spectroscopy Database, Version 4.1 (National Institute of Standards and Technology, Gaithersburg), http://srdata.nist.gov/xps/ (accessed: December 2015).

[19] Y. Huang, J. Wu, X. Xu, Y. Ho, G. Ni, Q. Zou, G. Koon, W. Zhao, A. H. Castro Neto, G. Eda, C. Shen, B. Özyilmaz, *Nano Res.* **2013**, *6*, 200.